Landslides (2015) 12:1131–1138
DOI 10.1007/s10346-014-0532-7
Received: 5 September 2013
Accepted: 21 October 2014
Published online: 6 November 2014

H. Y. Chen · P. Cui · X. Q. Chen · X. H. Zhu · Gordon G. D. Zhou

Laboratory experiments of water pressure loads acting on a downstream dam caused by ice avalanches

Abstract A worldwide decline of mountain glaciers is occurring due to the impacts from climate warming. The retreat of mountain glaciers often leads to different kinds of geo-hazards. Serious surges triggered by glacier avalanches often pose a potential threat to the stability of dams. In this article, four different types of blocks with a constant density of about 900 kg/m^3 were used to simulate the glacier avalanches in natural conditions. By considering the raw material properties of the plate and blocks themselves, the plunging velocity of a block was calculated by a theoretical method instead of by video cameras. The effect of the slope angle, distance between the sliding block and the water surface, initial water depth, slide Froude number, geometry, and distance between the plunging point of the sliding blocks and the downstream dam was considered to study the characteristics of the pressure loads acting on the moraine dam. In addition, an empirical equation was obtained to predict the maximum pressure load acting on the dam. Pressure load on the glacier dam is only one of the crucial factors for dam safety analyses. The failure process of a moraine dam, the probable maximum discharge of outburst floods, and the transportation of sediments along the downstream valley should also be considered in future studies.

Keywords Glacier avalanches · Pressure load · Surge wave · Glacial lake · Moraine dam

Notation

The following symbols are used in this paper:

f	Friction coefficient with lubrication (−)
f'	Friction coefficient without lubrication (−)
g	The acceleration due to gravity (m/s^2)
h	Elevation between a block and the water surface (m)
h_o	Water depth of the dammed lake (m)
L	Sliding distance between the block and water surface (m)
L_m	Length of Midui lake in the model (m)
L_p	Length of Midui lake in the prototype (m)
L_1	Distance between the plunging point and the downstream dam (m)
M_s	The weight of the metal shell (kg)
M_f	The weight of the block (kg)
P	Pressure load at Pi (i=1, 2, 3, 4, 5) (kPa)
ΔP	The pressure difference between the maximum pressure and the minimum pressure at a given time (kPa)
P_{Max}	The maximum pressure load (kPa)
Pi	Testing point (i=1, 2, 3, 4, 5) (−)
S	The projected area on the flat plate (m^2)
t	Release time (s)
T	Period of a wave (s)
v_t	Plunging velocity of a block (m/s)
V	The volume of a block (0.024 m^3)
V_d	The volume of the diesel oil (m^3)
V_g	The volume of the gasoline (m^3)
V_m	The volume of the ice glacier in the model (m^3)
V_p	The volume of the ice glacier in the prototype (m^3)
W_m	The width of Midui lake in the model (m)
W_p	The width of Midui lake in the prototype (m)

Greek letters

α	Slope angle (°)
α'	The radian of the slope angle (−)
ρ_d	The density of diesel oil (830 kg/m^3)
ρ_g	The density of gasoline (730 kg/m^3)
ρ_m	The mean density of a block (900 kg/m^3)
ρ_s	The density of sliding block (kg/m^3)
ρ_w	The density of water (1000 kg/m^3)
μ	Water dynamic viscosity (Pa•s)

Introduction

Climatic warming leads to the retreat of glaciers in the high-mountain areas of the world. The associated geo-hazards include glacier avalanches, landslides, snow avalanches, rock falls, and so on. Surges may be generated when the phenomena above occur in the regions where confined water bodies such as moraine-dammed lakes, glacier-dammed lakes, reservoirs, and bays are impacted by ice or rock avalanches (Walder and Costa 1996; Clague and Evans 2000; Fritz et al. 2003a; Lipovsky et al. 2008; Lee et al. 2009; Allen et al. 2011). A famous moraine-dammed lake outburst event caused by the glacier avalanches in China was the Midui moraine-dammed lake which occurred on July 15, 1988. It was reported that an ice glacier with a volume of about 36×10^4 m^3 slid into the Midui moraine-dammed lake. The surge generated by the ice glacier led to the increasing of water level about 1.4 m and at last resulting in outburst of the lake (You and Cheng 2005).

Much attention has been paid to the characteristics of surges because a number of adverse outcomes are related to the surge-induced waves (Cui et al. 2010). In fact, a wave generated by the sliding block itself has little effect on the hydraulic structures or the bank of a lake. But the pressure load acting on a dam and overtopping of the dam may lead to total or partial dam break when a wave propagates up to the upstream face of the dam. The catastrophic dam-break floods from the confined water bodies seriously threaten the human life and public and private properties in these areas. The characteristics of an impulsive wave mainly consist of the amplitude, period, and energy. Experimental studies indicated that the parameters above were determined by a number of variables such as the plunging velocity, water depth, slope angle, mass of a sliding block, initial position, and shape of the sliding blocks (Panizzo et al. 2002; Fritz et al. 2003b; Panizzo et al. 2005;Ataie-Ashtiani and Najafi-Jilani 2008; Heller et al. 2008).

Using a video camera, surge waves induced by landslides in the near field were recorded and analyzed. It indicated that different

shoreline shapes were modified in different ways depending on how the landslides entered the water (Di Risio et al. 2009). In addition to the detailed description provided for the wave propagation in the reservoir, empirical equations were obtained to predict the first and second impulsive wave heights (Cui and Zhu 2011). In these studies, slide masses which generated the impulsive waves had high densities (e.g., landslides and rock falls). However, little attention has been paid to impulsive waves generated by low-density materials (e.g., glacier avalanches and snow avalanches).

Pressure load is one of the most important parameters which affect dam safety. A gravity concrete dam may be subject to fatigue failure when the pressure load acts on the dam periodically (Holmen 1982; Cornelissen and Reinhardt 1984; Slowik et al. 1996). Especially, the natural frequency of a dam itself is close to the periodic oscillation of the pressure load wave. However, in many cases, the dams such as a landslide dam, a glacier dam, or a moraine dam are formed by an unconsolidated, poorly sorted rock debris or highly heterogeneous mixture of particles (Meyer et al. 1994; Clague and Evans 2000; Dunning et al. 2006; Korup and Tweed 2007; Duman 2009; Kong et al. 2009; Cui et al. 2010; Cui et al. 2012). The pressure load acting on this type of dams may lead to changes of the pore water pressure or the stress structures in the dams. However, most of the relevant work has been focusing on investigating the characteristics of the impulse water wave, while little work has been conducted to study the variation of the pressure load acting on the dams (de Carvalho and Antunes do Carmo 2009).

In this study, experiments were conducted to study the characteristics of the water pressure loads acting on the dam. In the experiments, impulse waves were generated by different shapes of rigid sliding bodies with a specific volume. For each experimental test, video cameras were employed to record the sliding process of the rigid block along the flat plate. The effect of the main parameters such as the slope angle, distance between the sliding block and the water surface, and initial water depth was considered. An empirical equation was obtained to predict the maximum pressure load acting on the dam.

Design and fabrication of simulated experiments

Experimental setup

The experiments were performed on a debris fan of the Dawazi Gully, which is located near the Dongchuan Debris Flow Observation and Research Station (DDFORS), in Dongchuan District, Yunnan Province in China. Generally, a glacier lake which can result in hazards downstream is quite large. Therefore, it is difficult to build a large-scale model under the experimental condition. The model scale in the experiment was about 1:250. Although the model scale seemed to be small, the physical phenomena, such as surges generation, propagation of surge wave, were well uncovered in the experiments. The dimensions of the tank and blocks were based on outburst event of the Midui moraine-dammed lake. The characteristics of the prototype and modeled lake are shown in Table 1. The experimental setup consisted of a sliding block, an inclined plate with adjustable slopes, a dammed lake, and a downstream dam (Fig. 1). A series of pressure sensors was set on the downstream dam to monitor the pressure loads induced by the impulse waves. The inclined plate was about 3.5 m in length and 0.8 m in width, with adjustable slopes ranging from 30 to 46°.

Experiment design

In order to simulate a surge generated by a glacier, the density of the sliding blocks was consistent with that of the glacier, which was about 900 kg/m^3. In fact, it is very difficult to find a material with exactly the same density as the glacier in its natural form. In this article, the glacier was simulated by blocks made of light fluid materials (such as diesel or gasoline). First, a block with certain volume was made (V=0.024 m^3) with sheet iron. Then, mixed fluids composed of diesel and gasoline with different concentrations (ρ_g=730 kg/m^3; ρ_d=830 kg/m^3) were filled into the block in order to make the density of the block to be approximately equal to 900 kg/m^3. Four shaped blocks were designed as shown in Fig. 2. Although the first three blocks B1, B2, and B3 looked similar, the projected area S was different from each other when they block slid into water along the plate. For the first three blocks, we may find out whether the projected area S affects the pressure load exerted on the dam under the similar plunging type or not. B4 was considered in the experiment because its structure was different from the first three blocks. The main parameters of the blocks are shown in Table 2. All 64 tests were arranged according to the different values of each variable (Table 3).

Experiment results and discussion

Typical surge propagation and induced pressure loads

The process of the block sliding and wave propagation was recorded by video cameras. Figure 3a showed the initial status of the dammed lake. A surge was firstly triggered and propagated around when the block slid into the lake rapidly. The block was submerged initially and quickly rose up to the water surface due to the buoyancy force since its density was lower than that of the water. Another wave-induced surge occurred after the submerged block re-emerged in the dammed lake. Thus, at least two surges were observed to propagate downstream and towards the lateral bank of the dammed lake as shown in Fig. 3b. The block rose up to the water surface again as shown in Fig. 3c. Surges reflected from the bank resulted in oscillations of the block. Meanwhile, new surges were triggered when the block oscillated up and down at the water surface. During the process, the energy of the surge dissipated due to the water viscosity and friction between the water and solid boundary conditions (i.e., the bank and bed of the lake). It lasted a long time before the entire water body calmed down completely. The wave-induced pressure loads acting on the dam were monitored precisely by the

Table 1 Characteristics of the prototype and modeled lake (model scale 1:250)

Prototype sizes for the Midui moraine-dammed lake and ice glacier			Model sizes for the Midui moraine-dammed lake and ice glacier		
Length of Midui lake L_p (m)	Width of Midui lake W_p (m)	Volume of the ice glacier V_p (m^3)	Length of Midui lake L_m (m)	Width of Midui lake W_m (m)	Volume of the ice glacier V_m (m^3)
950	550	36×10^4	3.9	2.2	0.024

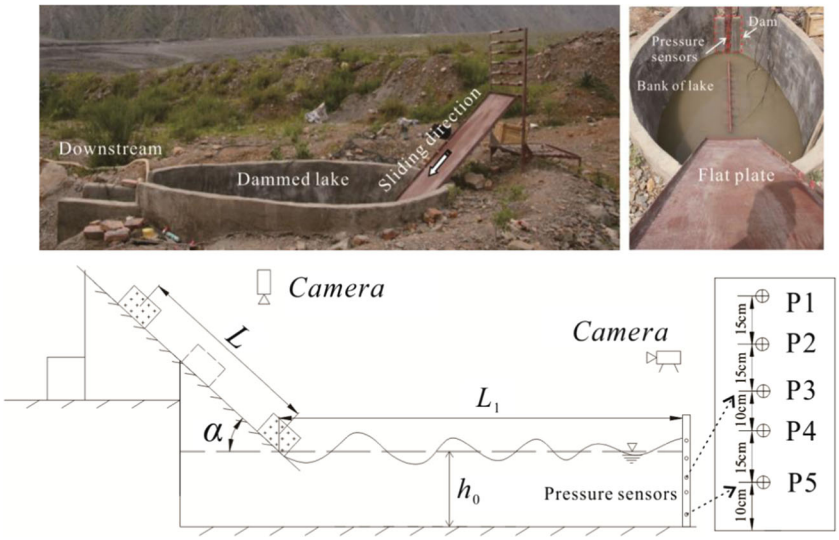

Fig. 1 Experiment setup

pressure sensors installed on the dam. A typical variation of the pressure loads at the testing points was shown in Fig. 4. It indicated that a surge triggered by a sliding block from an inclined flat plate affected the pressure loads on the dam from the bottom to the top. Generally, synchronized pressure loads at P*i* (*i*=1, 2, 3, 4, 5 in Fig. 4) were measured by the pressure sensors, with similar amplitudes and periods. ΔP was defined as the pressure difference between the maximum pressure and the minimum pressure at a given time. Figure 4 indicates that when *t*=24.30 s, ΔP at P1 and P5 was 0.69 and 0.39, respectively. When *t*=46.60 s, ΔP at P1 and P5 was 0.23 and 0.25, respectively. ΔP at P1 decreased by 66.5 % during the attenuation process. But ΔP at P5 decreased by 35.9 % during the attenuation process. The pressure amplitude around the water surface attenuated fast. However, the attenuation of the pressure amplitude near the bottom was slow because the turbulence at the water surface was stronger than that at deeper locations.

Characteristics of pressure loads for specific parameters

Typical parameters were considered to analyze the characteristics of the pressure loads at the testing points. Figure 4 shows that the variation of pressure loads at P1 was quite different from those at P*i* (*i*=2, 3, 4, 5), which was also strongly affected by the subsequent reflected water waves. Therefore, the variation of pressure loads at P2 was selected as a typical one to analyze the characteristics of the pressure loads acting on the downstream dam. In order to exclude the effect of surge reflection on the pressure load wave, we focused our attention on the first peak during the attenuation process, namely, when the first surge wave reached the testing points. It indicated that when *L*=1.7 m, the pressure load was about 1.84 kPa. When *L*=2.1 m, the pressure load reached 2.12 kPa. With increasing the sliding distance, the pressure load increased (Fig. 5a). As for the inclination angle, the minimum pressure load occurred when the inclination angle was about 41°. When the block slipped into the water with a relatively small inclination angle (α=30°), it drove the water on the top to move downstream directly, and the pressure load reached a peak value (A_1=2.1 kPa) before the surge reflected. When the inclination angle was relatively large (α=46°), although the sliding block did not drive the water to move downstream directly, it plunged into the lake at a larger velocity. As a result, surges with more energy were triggered, which resulted in an increase of pressure load. In addition, the pressure load reached an even higher value after the wave reflecting (A_2=2.2 kPa) (Fig. 5b). As far as the projected area *S* was concerned, the maximum pressure load for the first three blocks nearly reached the same value (about 2.2 kPa). The maximum pressure load of B4 which had the maximum projected area *S* (*S*=1416.3 cm^2) was a little smaller than that of the former three blocks (about 2.1 kPa) (Fig. 5c). The results indicated that the structure and the projected area of a block had slight effect on the pressure load.

Velocity determination

The velocity of the sliding block is a very important dynamic parameter when the pressure loads acting on a dam are considered. Researchers have put great effort in finding useful methods to determine the value of this parameter. The

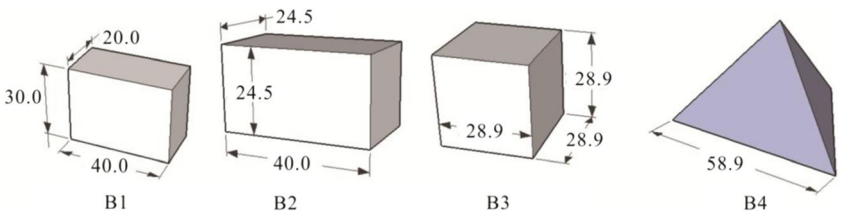

Fig. 2 Four types of blocks and their dimensions (in cm)

Table 2 Main parameters of the blocks

No.	V (m^3)	M_s (kg)	V_d (m^3)	V_g (m^3)	ρ_d (kg/m^3)	ρ_g (kg/m^3)	M_f (kg)	ρ_m (kg/m^3)
B1	0.0240	3.00	0.0108	0.0132	830.0	730.0	18.60	900.00
B2	0.0240	2.95	0.0114	0.0126	830.0	730.0	18.67	900.14
B3	0.0241	2.98	0.0112	0.0129	830.0	730.0	18.74	899.86
B4	0.0241	3.44	0.0065	0.0176	830.0	730.0	18.23	899.84

friction coefficient was minimized by lubricating the sliding surfaces and calculated from Eq.(1) when v_t was obtained by analyzing the video of the sliding process (Ataie-Ashtiani and Nik-Khah 2008; Najafi-Jilani and Ataie-Ashtinai 2008; Cui and Zhu 2011).

The friction coefficient f can be expressed as follows:

$$f = \left(g\sin\alpha - \frac{v_t}{t}\right) \Big/ (g\cos\alpha) \tag{1}$$

where g is the acceleration due to gravity, α is the slope angle, v_t is the plunging velocity of sliding block, and t is the release time.

Using video cameras to record the movement of the sliding block along a plate is a good way to analyze the velocity of the block. The velocity calculated here, however, is still an average velocity even if the release time is short. It is difficult to obtain the real value of the velocity when the block plunges into the water. In this article, the plunging velocity was calculated by a theoretical method by considering the raw material properties of the plate and the blocks. f was assumed to be the coefficient of kinetic friction between the sliding block and the steel plate. It is well known that the coefficient of kinetic friction f between different materials is mainly determined by the type of the raw material and the surface roughness. Table 4 shows that the coefficient of kinetic friction f' without lubrication varied from 0.15 to 0.18. Therefore, f' was assumed to be equal to 0.15 in the experiments for the flat plate and the sliding blocks which were both made of steel. It was dramatically different from the sliding block which was made of concrete block. In some cases, the average value of friction coefficient f' was about 0.413 (Cui and Zhu 2011).

The plunging velocity v_t was calculated as follows:

$$v_t = \sqrt{2gL\sin\alpha(1 - 0.15\cot\alpha)} \tag{2}$$

where L is the sliding distance between the block and water surface, g is the acceleration due to gravity, and α is the slope angle.

Comparison of the theoretical plunging velocities and the experimental values according to the video recordings is given in Table 5. It indicated that generally, the theoretical velocities were slightly higher than the experimental value. The minimum and maximum absolute error was about 0.60 and 13.33 %, respectively. The discrepancy between the theoretical and experimental values can be explained as follows: firstly, the plunging velocity calculated in theory was under ideal conditions, namely, the coefficient of

Table 3 Initial conditions for each run

Types of sliding block	Sliding distances (m)			
	α=30°	α=36°	α=41°	α=46°
B1	2.90	2.70	2.60	2.50
	2.50	2.30	2.20	2.10
	2.10	1.90	1.80	1.70
	1.70	1.50	1.40	1.30
B2	2.90	2.70	2.60	2.50
	2.50	2.30	2.20	2.10
	2.10	1.90	1.80	1.70
	1.70	1.50	1.40	1.30
B3	2.90	2.70	2.60	2.50
	2.50	2.30	2.20	2.10
	2.10	1.90	1.80	1.70
	1.70	1.50	1.40	1.30
B4	2.90	2.70	2.60	2.50
	2.50	2.30	2.20	2.10
	2.10	1.90	1.80	1.70
	1.70	1.50	1.40	1.30

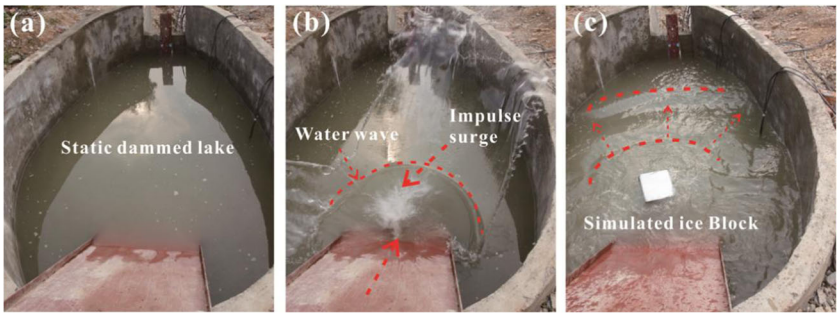

Fig. 3 Typical process of wave propagation (B1; α=30°; L=2.90 m)

kinetic friction on the whole plate was assumed to be constant. However, in the experiment, it was difficult to keep the coefficient of kinetic friction constant due to the flatness of the plate and the block surfaces. Secondly, the so-called plunging velocity obtained by the video recordings (experimental velocity) was actually the average velocity. No matter how big the time interval was, the experimental velocity was undoubtedly smaller than the instantaneous velocity when the block plunges into water.

Empirical equation for predicting pressure loads on the dam

Generally, the pressure loads caused by surges are determined by the volume of the sliding block V, sliding angle α, sliding distance L, density of the sliding block ρ_s, water density ρ_w, water depth h_o, water dynamic viscosity μ, and distance between the sliding point and the dam L_1 (Kamphuis and Bowering 1972; Panizzo et al. 2002). It is a very complicated problem if all the physical parameters above are considered in the experiments. This study neglected some constants and added some important parameters that strongly affected the characteristics of a surge.

The maximum pressure load P_{Max} is mainly determined by the parameters as follows:

$$P_{Max} = f(\rho_w, g, L, V, S, L_1, h_o, \alpha) \tag{3}$$

where ρ_w is the density of water, g is the acceleration due to gravity, L is the sliding distance between the block and water surface, V is the volume of a block (0.024 m^3), L_1 is the distance between the plunging point and the downstream dam, h_o is the water depth of the dammed lake, α is the slope angle, and S is the projected area

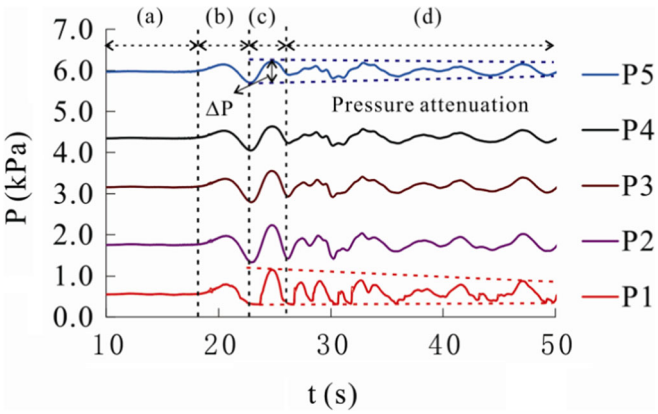

Fig. 4 Typical fluctuation of pressure loads (B4; α=46°;L=2.50 m): *a* still dammed lake before the block slid into the lake, *b* surge propagation and reflected wave from the bank, *c* secondary surge propagation, and *d* pressure loads attenuation. The initial depth of the dammed lake was fixed at a value of 0.7 m

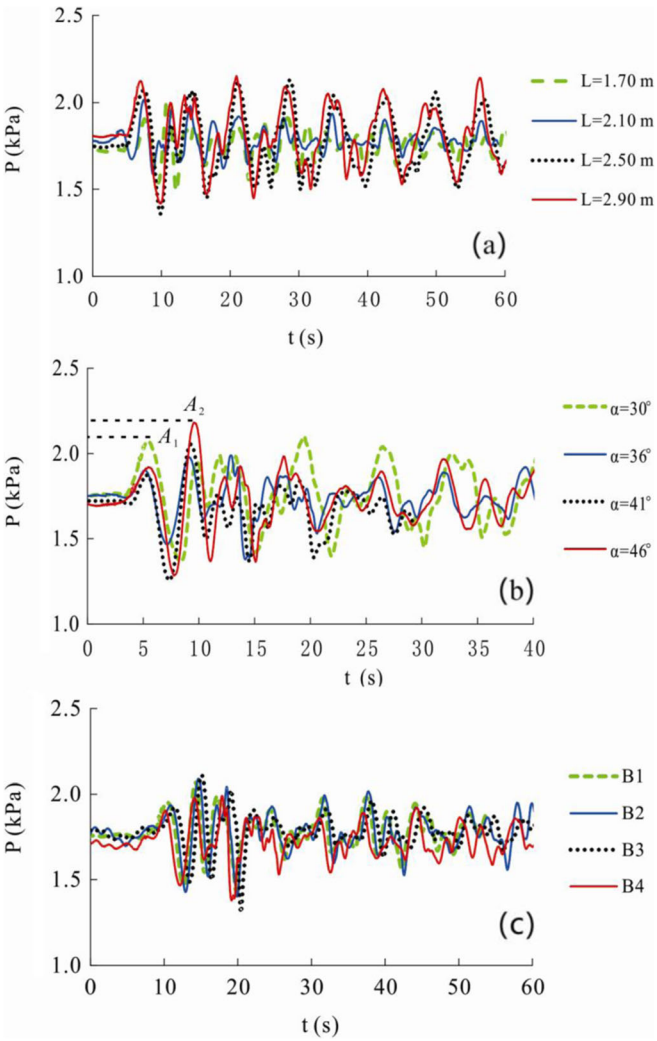

Fig. 5 Characteristics of pressure loads for different factors at P2 (B4): **a** pressure loads induced by sliding block with different sliding distances. It indicates that generally, increasing the sliding distance increases the pressure loads when the other parameters were fixed. **b** Pressure loads induced by sliding block at different sliding slopes. It indicates that increasing the sliding slope causes the maximum pressure load to decrease first and then increase. **c** Pressure loads induced by sliding block in different blocks

Table 4 Coefficient of kinetic friction f' between different materials

Items	Coefficient of kinetic friction		
Materials	Steel-steel	Steel-cast iron	Cast iron-cast iron
With lubrication f	0.05~0.1	0.05~0.15	0.07~0.12
Without lubrication f'	0.15	0.18	0.15

on the plane which is perpendicular to the plate, namely, the maximum area at the cross section.

Based on the dimensional analysis, the dimensionless parameters with clear physical meaning were developed as follows:

$$\frac{P_{Max}}{\rho_w g h_0} = f\left(\frac{L}{L_1}, \frac{V}{Sh_0}, \frac{v_t}{\sqrt{gh_0}}, \alpha'\right) \tag{4}$$

where v_t is the plunging velocity, L/L_1 is the dimensionless sliding distance, V/Sh_0 is the dimensionless volume of the blocks, $F_r = v_t/\sqrt{gh_0}$ is the sliding Froude number, and α' is the radian of the inclined angle. The dimensionless parameters V/Sh_0, $F_r = v_t/\sqrt{gh_0}$, and α' are considered to be the key parameters when studying the impact of different types of solid materials on the water body. As for the pressure loads exerted on the dam, the dimensionless sliding distance L/L_1 should be considered due to the attenuation of the impulse water wave propagating downstream.

A regression equation was developed based on a series of test data with α ranging between 36 and 46° as shown in Table 3.

$$\frac{P_{Max}}{\rho_w g h_0} = 0.0386\left(\frac{L}{L_1}\right)^{-0.2831}\left(\frac{V}{Sh_0}\right)^{0.0963}\left(\frac{v_t}{\sqrt{gh_0}}\right)^{1.2207}\alpha'^{0.4596} \tag{5}$$

The regression equation above demonstrated that the dimensions of the blocks had slight effect on the pressure load. Although there was a positive correlation between the sliding distance and the pressure load, L_1 affected the amount of the wave energy which determined the pressure loads acting on the dam. Therefore, it had only slight effect on the pressure load. The sliding Froude number F_r which was mainly determined by the sliding distance had the strongest effect on the pressure load. In addition, the sliding slope also appeared to have some effect on the pressure load. The rest of the test data were applied to verify the reliability of the regression equation (when α ranged between 30 and 41°). The results indicated that the maximum error is about 33.3 % and most errors were below 15 % (Fig. 6). Therefore, the regression equation can be used to estimate the maximum pressure load if no better method is available. Errors existing between the predicted data and the experimental ones are explained as follows: First, precision will be affected by the parameters the authors have chosen. Second, equipment error or human error with respect to measurement

Table 5 Comparison of theoretical velocities and experimental data (e.g. B1)

Slope angle	Distances (m)	Theoretical velocity (m/s)	Experimental velocity (m/s)	Error (%)
α=30°	2.90	4.59	4.46	−2.83
	2.50	4.26	3.91	−8.22
	2.10	3.90	3.38	−13.33
	1.70	3.51	3.05	−13.11
α=36°	2.70	4.97	5.00	0.60
	2.30	4.59	4.46	−2.83
	1.90	4.17	3.91	−6.24
	1.50	3.70	3.47	−6.22
α=41°	2.60	5.26	5.43	3.23
	2.20	4.84	4.63	−4.34
	1.80	4.38	4.17	−4.79
	1.40	3.86	3.91	1.30
α=46°	2.50	5.49	5.68	3.46
	2.10	5.03	4.81	−4.37
	1.70	4.53	4.46	−1.55
	1.30	3.96	3.57	−9.85

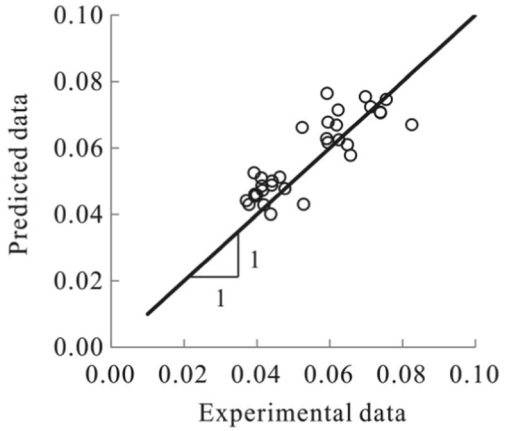

Fig. 6 Comparison of predicted data and experimental ones

results in decreased precision. Further study will be carried out to verify the validation of the regression equation in the future.

Discussion

This article described an experimental investigation on the pressure loads acting on the downstream dam. However, the experiments were performed under ideal conditions. The sliding blocks in the experiments were rigid. In reality, the glacier will melt gradually when it slides into a dammed lake. Therefore, the variations of the pressure loads will become more complex when the melting process is considered. Additionally, some other problems such as the failure process of the moraine dam, the probable maximum discharge of outburst floods, and the transportation of sediments along the downstream valley should be considered in future studies to better understand the failure mechanisms of moraine-dammed lakes and their secondary hazards.

Conclusions

The characteristics of the pressure loads acting on the downstream dam induced by surges were investigated in the experiments. Four types of sliding blocks were designed to simulate the glacier avalanches under natural conditions. An empirical equation with clear physical meaning was developed to predict the maximum pressure load. Conclusions were drawn as follows:

1. It was found that increasing the sliding distance resulted in the increase of the maximum pressure load. However, increasing the sliding slope caused the maximum pressure load to decrease first and then increase. In addition, the attenuation speed of ΔP was different from bottom to top. With decreasing the net water depth, the attenuation speed of ΔP increased due to the violent turbulence at the water surface.
2. By considering the raw material properties of the plate and the blocks, the plunging velocity of a sliding block was estimated. The comparison of the theoretical velocities and experimental values indicated that the estimated velocities were more suitable to represent the real value of the plunging velocity when the blocks plunged into water.
3. An empirical equation was developed to predict the maximum pressure loads acting on the dam based on the results of 32 tests. The results indicated that most errors were below 15 %. So, the regression equation could be used to estimate the maximum pressure load if no better method was available. The errors were mainly determined by the parameters the authors had chosen. In addition, equipment error or human error with respect to measurement resulted in decreased precision.
4. Serial surge waves were generated when a sliding block slid into water. Except the first surge wave, the following ones were affected by the waves reflected from sidewalls of the tank. The properties of the pressure loads were also affected by the spurious effect correspondingly. So, more detailed investigation of the properties of the surge waves and pressure loads will be conducted by using a larger tank in the future.

Acknowledgments

The research work was supported by the National Natural Science Foundation of China(Grant No. 41030742,41190084,51209195), the Youth Foundation of the Institute of Mountain Hazards and Environment, CAS (Grant No. SDS-QN-1302), and Foundation of Key Laboratory of Mountain Hazards and Earth Surface Process, Chinese Academy of Sciences.

References

Allen SK, Cox SC, Owens IF (2011) Rock avalanches and other landslides in the central Southern Alps of New Zealand: a regional study considering possible climate change impacts. Landslides 8(1):33–48

Ataie-Ashtiani B, Najafi-Jilani A (2008) Laboratory investigations on impulsive waves caused by underwater landslide. Coast Eng 55(12):989–1004

Ataie-Ashtiani B, Nik-Khah A (2008) Impulsive waves caused by subaerial landslides. Environ Fluid Mech 8(3):263–280

Clague JJ, Evans SG (2000) A review of catastrophic drainage of moraine-dammed lakes in British Columbia. Quat Sci Rev 19(17–18):1763–1783

Cornelissen HAW, Reinhardt HW (1984) Uniaxial tensile fatigue failure of concrete under constant-amplitude and programme loading. Mag Concr Res 36:216–226

Cui P, Zhu XH (2011) Surge generation in reservoirs by landslides triggered by the Wenchuan earthquake. J Earthq Tsunami 5(5):461–474

Cui P, Dang C, Cheng ZL et al (2010) Debris flows resulting from glacial-lake outburst floods in Tibet, China. Phys Geogr 31(6):508–527

Cui P, Dang C, Zhuang JQ et al (2012) Landslide-dammed lake at Tangjiashan, Sichuan Province, China (triggered by the Wenchuan earthquake, May 12, 2008): risk assessment, mitigation strategy, and lessons learned. Environ Earth Sci 65:1055–1065

de Carvalho RF, Antunes do Carmo JS (2009) Landslides into reservoirs and their impacts on banks. Environ Fluid Mech 7(6):481–493

Di Risio M, Bellotti G, Panizzo A, De Girolamo P (2009) Three-dimensional experiments on landslide generated waves at a sloping coast. Coast Eng 56(5–6):659–671

Duman TY (2009) The largest landslide dam in Turkey: Tortum landslide. Eng Geol 104(1–2):66–79

Dunning SA, Rosser NJ, Petley DN, Massey CR (2006) Formation and failure of the Tsatichhu landslide dam, Bhutan. Landslides 3(2):107–113

Fritz HM, Hager WH, Minor HE (2003a) Landslide generated impulse waves. 1. Instantaneous flow fields. Exp Fluids 35(6):505–519

Fritz HM, Hager WH, Minor HE (2003b) Landslide generated impulse waves. 2. Hydrodynamic impact craters. Exp Fluids 35(6):520–532

Heller V, Hager WH, Minor HE (2008) Scale effects in subaerial landslide generated impulse waves. Exp Fluids 44(5):691–703

Holmen JO (1982) Fatigue of concrete by constant and variable amplitude loading. Fatigue Concr Struct 75:71–110

Kamphuis JW, Bowering RJ (1972) Impulse waves generated by landslides. Proc. 12th Coastal Eng. Conf.:575–588

Kong P, Na C, Fink D, Zhao X, Xiao W (2009) Moraine dam related to late Quaternary glaciation in the Yulong Mountains, southwest China, and impacts on the Jinsha River. Quat Sci Rev 28(27–28):3224–3235

Korup O, Tweed F (2007) Ice, moraine, and landslide dams in mountainous terrain. Quat Sci Rev 26(25–28):3406–3422

Lee J, Davies T, Bell D (2009) Successive Holocene rock avalanches at Lake Coleridge, Canterbury, New Zealand. Landslides 6(4):287–297

Lipovsky PS, Evans SG, Clague JJ, Hopkinson C et al (2008) The July 2007 rock and ice avalanches at Mount Steele, St. Elias Mountains, Yukon. Can Landslides 5(4):445–455

Meyer W, Schuster RL, Sabol MA (1994) Potential for seepage erosion of landslide dam. J Geotech Eng 120(7):1211–1229

Najafi-Jilani A, Ataie-Ashtinai B (2008) Estimation of near field characteristics of tsunami generation by submarine landslide. Ocean Eng 35(5–6):545–557

Panizzo A, Bellotti G, De Girolamo P (2002) Application of wavelet transform analysis to landslide generated waves. Coast Eng 44(4):321–338

Panizzo A, de Girolamo P, Di Risio M, Maistri A, Petaccia A (2005) Great landslide events in Italian artificial reservoirs. Nat Hazards Earth Syst Sci 5(5):733–740

Slowik V, Plizzari GA, Saouma VE (1996) Fracture of concrete under variable amplitude fatigue loading. ACI Mater J 93(3):272–283

Walder JS, Costa JE (1996) Outflow floods from glacier-dammed lakes: the effect of mode of lake drainage on flood magnitude. Earth Surf Process Landf 21(8):701–723

You Y, Cheng ZL (2005) Modeling experiment of debris flow in Midui Gully, Tibet. J Mt Sci 23(3):289–293

H. Y. Chen · P. Cui (✉) · X. Q. Chen · X. H. Zhu · G. G. D. Zhou
Key Laboratory of Mountain Hazards and Earth Surface Processes, CAS/Institute of Mountain Hazards and Environment, CAS,
Chengdu, 610041, China
e-mail: pengcui@imde.ac.cn

H. Chen
e-mail: hychen@imde.ac.cn

P. Cui
CAS Center for Excellence in Tibetan Plateau Earth Sciences,
Beijing, 100101, China